

MIMO Radar – Waveforms and Applications

B. J. Donnet, I. D. Longstaff
Filtronic Pty Ltd,
2/205 Queensport Road, Murarrie 4172, Queensland, Australia

Abstract

This paper describes two applications suited to the particular characteristics of MIMO radar. We provide a brief description of the MIMO radars which could meet these applications and present a detailed analysis of two candidate waveform types suited to these applications. Each of the waveform types are shown to have different characteristics that make them better suited to one application area over the other.

Keywords: MIMO radar, phased array radar, radar applications, radar signals, radar signal processing

Introduction

Waveform selection plays a critical role in determining the suitability of MIMO radar for a given application. Two application areas have been identified where MIMO radar is thought to offer an advantage over conventional radar [1]. Both involve rapidly scanning a large volume, one searching for fast moving targets in clear air; the other, slow moving targets in clutter. This paper outlines the application areas and presents an analysis of two MIMO radar enabling waveform types.

Application areas where MIMO radar offers an advantage

During the course of the “MIMO Radar – Prospects and Constraints” DTC project, two application areas were identified where MIMO radar is believed to offer an advantage over conventional radar. Both application areas involve rapidly scanning a large volume, but for significantly different targets and environments.

The first application area is aimed at detecting slow moving targets in a cluttered environment. Current scanning radars for

this application need to compromise between the long dwell time required for Doppler processing and the fast scanning rate required for quick reaction times. MIMO radar offers the advantage of allowing the long dwell times required for target detection and clutter suppression, while maintaining continuous coverage of the entire volume.

The second application area is aimed at detecting fast moving targets in clear air. Here MIMO radar offers the angular resolution performance of much larger phased array radars for a fraction of the weight and cost. MIMO also enables continuous coverage of the entire volume, facilitating detection of targets that may be missed by scanning beam systems.

MIMO radars depend on transmitting orthogonal waveforms from each transmitter antenna element of the array, so allowing the returns to be separated on reception [1]. Typically M codes are required in the set, where M is the number of transmitter elements.

Costas codes applied to an OFDM waveform structure

Costas codes are Doppler tolerant frequency hopping waveforms that exhibit near-ideal range-Doppler ambiguity functions [2] (Figure 1). There are several methods for constructing Costas codes [3], with no one method able to generate all codes. The Costas codes analysed were generated using Welch-Costas construction, which is explained in detail in reference [4].

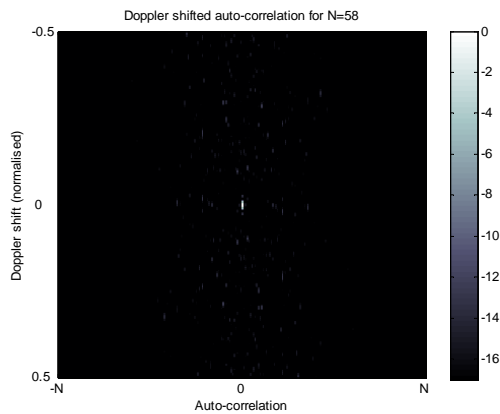


Figure 1 Costas code range-Doppler ambiguity function for $N=58$

Welch-Costas construction is based around finding “primitive roots” to a Galois field (finite number field) [4]. The number of elements N in the Galois field is one less than some prime number p . The primitive roots g of the Galois field are defined as the integers $1 \leq g \leq N$ that satisfy (1), generating all of the integers i between 1 and N .

$$i = g^j \text{ mod}(p), 1 \leq j \leq N \quad (1)$$

The sequence of integers generated by a given value of g corresponds to the Costas code of length N , generator g . The integer sequence represents the frequency hopping pattern of the Costas code.

The length and frequency separation of the hops is constructed using Orthogonal Frequency Division Multiplexing (OFDM), where the hop width is the reciprocal of the hop frequency separation [5, 6]. This

optimises bandwidth coverage whilst minimising inter-hop interference [6].

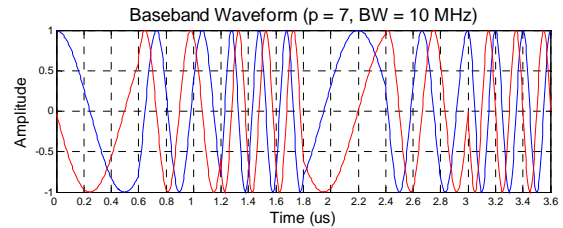


Figure 2 Complex baseband Costas code OFDM waveform (after [1])

Figure 2 shows an example I/Q baseband waveform for $p=7$ with 10 MHz bandwidth. The OFDM waveform construction generates a total of N^2 critical samples resulting in a code a gain of N^2 [6].

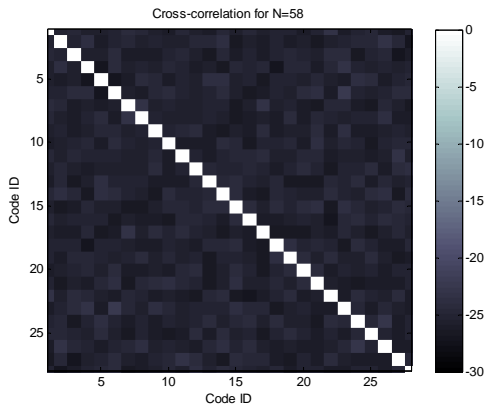
The length of the Costas code affects the cross-correlation properties, with Titlebaum and Maric [7] having proven that for Welch-Costas construction, a worst-case cross-correlation of $(p-1)/2$ occurs when:

$$p = 2e + 1 \quad (e \text{ is an even number}) \quad (2)$$

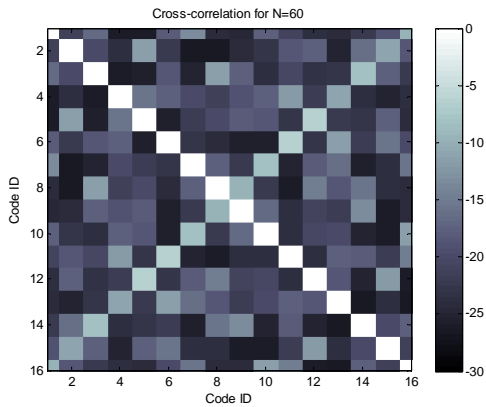
Titlebaum and Maric have also conjectured that Costas code sets generated using Welch-Costas construction have the least cross-correlation when p meets the criteria:

$$\text{prime}\left(\frac{p-1}{2}\right) = \text{true} \quad (3)$$

This is illustrated below in Figure 3 for adjacent primes. Figure 3(b) clearly shows the cross-correlation terms when (2) is satisfied; compared with Figure 3(a), which satisfies (3).



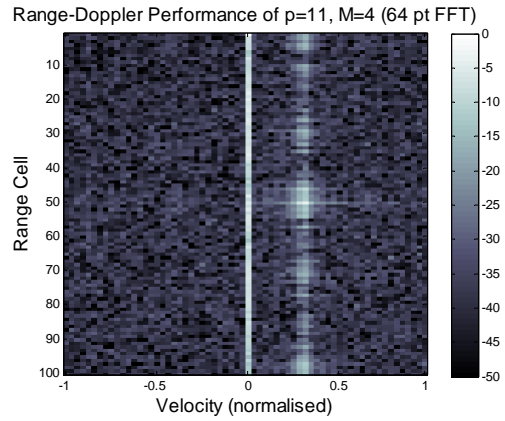
(a) $N=58$ ($p=59$; $(p-1)/2$ is prime)



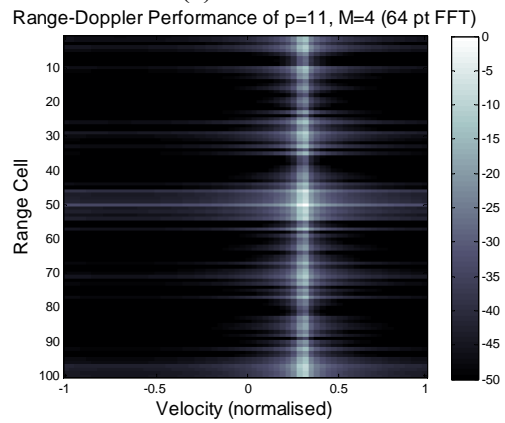
(b) $N=60$ ($p=61$; $p=2e+1$)

Figure 3 Cross-correlation of Costas codes

Costas codes are best suited to clear air applications [1]. The integrated sidelobe noise combined with long code lengths imposed by the OFDM waveform construction greatly reduces the sensitivity in a cluttered environment. Below, Figure 4 compares the normalised response of a simulated target with and without clutter. Figure 4(a) shows the target with clutter; and Figure 4(b) is the same target and waveform without clutter.



(a) With clutter



(b) Without clutter

Figure 4 Target response with and without clutter

The waveform used in Figure 4 has $N=10$, which satisfies (3) and on its own is expected to give a peak autocorrelation sidelobe of -20 dB. Four different codes of $N=10$ are used simultaneously, degrading the sidelobe performance by approximately 6 dB to -14 dB. The sidelobes in Figure 4(a) appear less dominant than in Figure 4(b) because they are partially masked by the clutter noise. The frequency axis of Figure 4 has been normalised to the Doppler ambiguity of the simulation.

Golay complementary pairs

Marcel Golay first proposed binary complementary series in [8] as a solution to an optical problem in multi-slit spectrometry. The premise of complementary codes is that the two codes have equal and opposite sidelobes that sum to zero. The desired autocorrelation peaks

both align, giving twice the gain with zero range sidelobes.

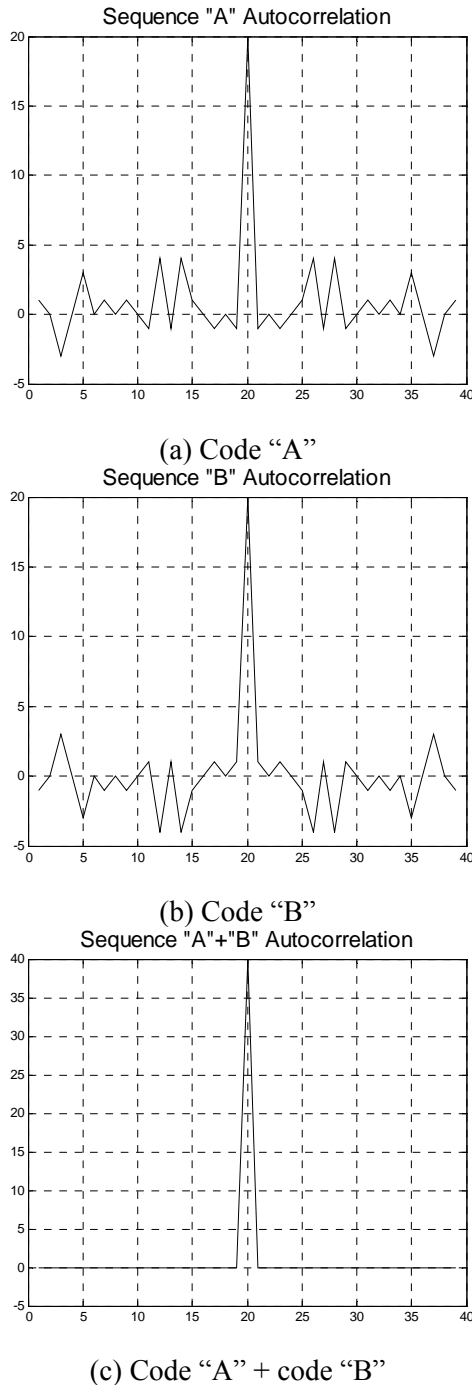


Figure 5 Golay complementary pair

There are several direct and recursive constructions that can be used to generate Golay complementary code pairs (GCP), detailed in [9, 10]. Valid lengths of GCPs can be expressed as $N=2^\alpha 10^\beta 26^\gamma$, where α , β and γ are integers ≥ 0 [10]. All GCPs can be constructed from a set of *primitive*

sequences of lengths 2, 10 and 26 and a set of six rules defining allowable equivalence permutations, given in [9].

Binary symbols are represented as either +1 or -1 and code pairs (A, B) are expressed in polynomial form:

$$a(z) = (a_0 + a_1 z + a_2 z^2 \dots a_{M-1} z^{M-1}) \quad (4)$$

Likewise for $b(z)$, with the coefficients representing the binary symbols. Two existing code pairs (A, B) and (C, D) of lengths M and N respectively are combined to form a code pair (X, Y) of length MN using the Turyn recursive construction [10]:

$$X(z) = a(z^N)(c(z) + d(z))/2 + z^{N(M-1)} b(z^N)(c(z) - d(z))/2 \quad (5)$$

$$Y(z) = b(z^N)(c(z) + d(z))/2 - z^{N(M-1)} a(z^N)(c(z) - d(z))/2 \quad (6)$$

Each code is used as a direct spreading sequence, with the range resolution bandwidth setting the chipping rate. Each code has a gain of N , where N is the code length, giving a total gain for the complementary pair of $2N$.

When using multiple codes simultaneously, which is desired in MIMO radar, it is important to select codes with minimum cross-correlation. There exists a sub-set of Golay complementary pairs that exhibit perfect isolation under ideal circumstances, called zero cross-correlation codes (ZCC) [11].

Analysis conducted by Wakasugi and Fukao [12] suggests that Golay complementary pairs are susceptible to degradation in the presence of Doppler. Figure 6 illustrates the degradation of a GCP code over Doppler shifts from 0% to 1% of the range resolution. From Figure 6 it can be seen that Doppler shifts of less than 0.1% of the range resolution bandwidth have little impact. To put this in context, 0.1% of 15 m range resolution at X-band equates to approximately 150 ms^{-1} .

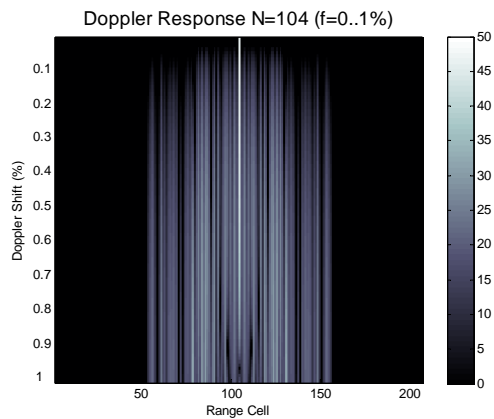


Figure 6 Degradation of GCP code in the presence of Doppler

The sidelobes of a GCP code are non-zero in the presence of clutter, as seen in Figure 7. However, the sidelobes are still much lower than the “ideal” Costas code sidelobes.

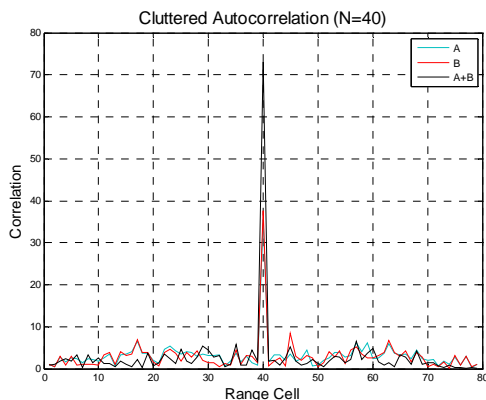
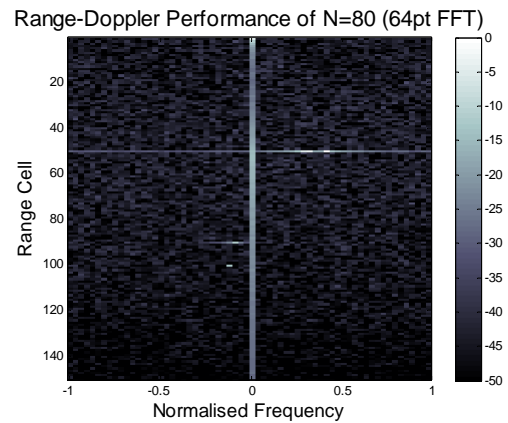
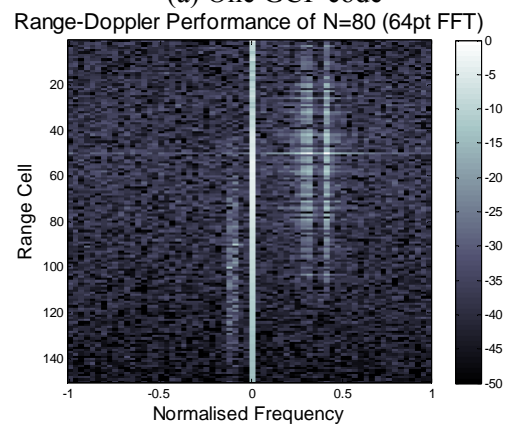


Figure 7 Degraded GCP code sidelobes in the presence of clutter

The GCP code is suitable for detecting slow moving targets in cluttered environments. Even when using multiple non-ZCC codes, Figure 8 shows that multiple targets that are of similar range and velocity can still be separated; and have sufficient peak to sidelobe ratio. In Figure 8(b), the peak to sidelobe ratio is approximately 15 dB.



(a) One GCP code



(b) Four GCP codes (non-ZCC)

Figure 8 Detection of multiple targets in clutter using GCP codes

Figure 8(a) shows that it is possible to effectively eliminate range sidelobes for applications where there is sufficient time to use only one transmitter. The frequency axis of Figure 8 has been normalised to the Doppler ambiguity of the simulation, which was set at 0.1% of the range resolution bandwidth.

Conclusion

Two application areas where MIMO radar offers an advantage over conventional radar have been presented. These are rapid volume scanning for fast moving targets in clear air; and slow moving targets in clutter.

Candidate waveform types for both applications have been assessed. It was shown that Costas codes applied to an OFDM waveform structure are suited to detecting fast moving targets in clear air.

The Golay complementary pair codes are suitable for detecting slow moving targets in cluttered environments.

A series of experiments will be conducted to validate the theoretical analysis presented in this paper. It is anticipated that the experiments will test both waveform types presented and verify the operational advantages offered by MIMO radar.

References

1. B. J. Donnet, *MIMO Radar – Prospects and Constraints: Detailed Analysis: WP3 Technical Deliverable*, Filtronic Pty Ltd, March 2007.
2. J. P. Costas, “A study of a class of detection waveforms having nearly ideal range-Doppler ambiguity properties”, *Proceedings of the IEEE*, pp 996-1009, Vol 72, No 8, August 1984.
3. K. Drakakis, “A review of Costas arrays”, *Journal of Applied Mathematics*, Vol 2006, Article ID 26385, 32 pages, 2006.
4. S. Rickard, “Searching for Costas arrays using periodicity properties”, *IMA International Conference on Mathematics in Signal Processing*, The Royal Agricultural College, Cirencester, December 2004.
5. B. J. Donnet, I. D. Longstaff, “Combining MIMO radar with OFDM communications”, *Proceedings of the 3rd European Radar Conference*, Manchester, England, pp 37-40, September 2006.
6. B. J. Donnet, I. D. Longstaff, “OFDM and pulse compression in MIMO radar”, *MIMO Radar – Prospects and Constraints: WP1 Technical Deliverable*, Filtronic Pty Ltd, pp 19-23, September 2006.
7. E. L. Titlebaum, S. V. Maric, “Multiuser sonar properties for Costas array frequency hop coded signals” *Proc. IEEE ICASSP 1990*, pp 2727–2730, 1990.
8. M. Golay, “Complementary Codes”, *Information Theory, IEEE Transactions on*, Volume 7, Issue 2, pp 82-87, April 1961.
9. P. B. Borwein, R. A. Ferguson, “A complete description of Golay pairs for lengths up to 100”, *Mathematics of Computation*, Volume 73, No 246, pp 967-985, 2004.
10. M. G. Parker, K. G. Paterson, C. Tellambura, “Golay Complementary Sequences”, www.isg.rhul.ac.uk/~kp/golaysurvey.pdf, 18 pages, January 2004.
11. K. Gerlach, F. F. Kretschmer, “General forms and properties of zero cross-correlation radar waveforms”, *Aerospace and Electronic Systems, IEEE Transactions on*, Volume 28, Issue 1, pp 98-104, January 1992.
12. K. Wakasugi, S. Fukao, “Sidelobe Properties of a Complementary Code Used in MST Radar Observations”, *Geoscience and Remote Sensing, IEEE Transactions on*, Volume GE-23, Issue 1, pp 57-59, January 1985.

Acknowledgements

The work reported in this paper was funded by the Electro-Magnetic Remote Sensing (EMRS) Defence Technology Centre, established by the UK Ministry of Defence and run by a consortium consisting of SELEX Sensors and Airborne Systems, Thales Defence, Roke Manor Research and Filtronic.